8-1-2016

Roles of mechanistic target of rapamycin and transforming growth factor-B signaling in the molting gland (Y-organ) of the blackback land crab, Gecarcinus lateralis

Ali M. Abuhagr
Colorado State University

Kyle S. MacLea
University of New Hampshire, Manchester, kyle.maclea@unh.edu

Megan R. Mudron
Colorado State University

Sharon A. Chang
University of California, Davis

Ernest S. Chang
University of California, Davis

See next page for additional authors

Recommended Citation

Abuhagr, A.M., MacLea, K.S., Mudron, M.R., Chang, S.A., Chang, E.S., and Mykles, D.L. Roles of mechanistic target of rapamycin and transforming growth factor-B signaling in the molting gland (Y-organ) of the blackback land crab, Gecarcinus lateralis. Comp Biochem Physiol A Mol Integr Physiol, 198:15-21. doi: 10.1016/j.cbpa.2016.03.018, 2016.

Roles of mechanistic target of rapamycin and transforming growth factor-β signaling in the molting gland (Y-organ) of the blackback land crab, *Gecarcinus lateralis*

Ali M. Abuhagr[1], Kyle S. MacLea[1 †], Megan R. Mudron[1], Sharon A. Chang[2], Ernest S. Chang[2], and Donald L. Mykles[1]*

[1]Department of Biology, Colorado State University, Fort Collins, CO 80523 USA

[2]Bodega Marine Laboratory, University of California-Davis, Bodega Bay, CA 94923 USA

Keywords: target of rapamycin; transforming growth factor-β; Activin; myostatin, Rheb; Akt; p70 S6 kinase; molting; Crustacea; Y-organ; ecdysteroid

[†]Current address: Department of Life Sciences, University of New Hampshire, Manchester, NH 03101 USA

*Corresponding author:

Dr. Donald L. Mykles
Department of Biology
Colorado State University
Campus delivery 1878
Fort Collins, CO 80523 USA

Office: 970-491-7616
Fax: 970-491-0649
E-mail: Donald.Mykles@ColoState.edu

ABSTRACT

Molting in decapod crustaceans is controlled by molt-inhibiting hormone (MIH), an eyestalk neuropeptide that suppresses production of ecdysteroids by a pair of molting glands (Y-organs or YOs). Eyestalk ablation (ESA) activates the YOs, which hypertrophy and increase ecdysteroid secretion. At mid premolt, which occurs 7-14 days post-ESA, the YO transitions to the committed state; hemolymph ecdysteroid titers increase further and the animal reaches ecdysis ~3 weeks post-ESA. Two conserved signaling pathways, mechanistic target of rapamycin (mTOR) and transforming growth factor-β (TGF-β), are expressed in the *Gecarcinus lateralis* YO. Rapamycin, an mTOR antagonist, inhibits YO ecdysteroidogenesis *in vitro*. In this study, rapamycin lowered hemolymph ecdysteroid titer in ESA *G. lateralis in vivo*; levels were significantly lower than in control animals at all intervals (1 to 14 days post-ESA). Injection of SB431542, an activin TGF-β receptor antagonist, lowered hemolymph ecdysteroid titers 7 and 14 days post-ESA, but had no effect on ecdysteroid titers at 1 and 3 days post-ESA. mRNA levels of mTOR signaling genes *Gl-mTOR*, *Gl-Akt*, and *Gl-S6k* were increased by 3 days post-ESA; the increases in *Gl-mTOR* and *Gl-Akt* mRNA levels were blocked by SB431542. *Gl-elongation factor 2* and *Gl-Rheb* mRNA levels were not affected by ESA, but SB431542 lowered mRNA levels at Days 3 and 7 post-ESA. The mRNA level of an activin TGF-β peptide, *Gl-myostatin-like factor* (*Mstn*), increased 5.5-fold from 0 to 3 days post-ESA, followed by a 50-fold decrease from 3 to 7 days post-ESA. These data suggest that (1) YO activation involves an up regulation of the mTOR signaling pathway; (2) mTOR is required for YO commitment; and (3) a Mstn-like factor mediates the transition of the YO from the activated to the committed state.

1. Introduction

Control of molting in crustaceans involves a complex interaction between the eyestalk neurosecretory center, which produces inhibitory neuropeptides, such as molt-inhibiting hormone (MIH) and crustacean hyperglycemic hormone (CHH), and a pair of molting glands (Y-organs or YOs) in the anterior cephalothorax (Chang and Mykles, 2011; Hopkins, 2012; Webster, 2015). MIH maintains the YO in the basal state during intermolt (stage C_4) through a cyclic nucleotide second messenger pathway (Chang and Mykles, 2011; Covi et al., 2009, 2012). A reduction in MIH activates the YO and triggers the transition from intermolt to premolt (stage D_0). Molting is induced by eyestalk ablation (ESA) or multiple leg autotomy in many decapod species, including *Gecarcinus lateralis* (Chang and Mykles, 2011; Mykles, 2001). The activated YO hypertrophies to increase molting hormone (ecdysteroids) synthetic capacity (Chang and Mykles, 2011; Mykles, 2011). The YO remains sensitive to MIH, CHH, and other factors, so that premolt processes can be temporally suspended by stress or injury (e.g., limb bud autotomy or LBA) (Chang and Mykles, 2011; Mykles, 2001; Nakatsuji et al., 2009; Yu et al., 2002). By mid premolt (stage $D_{1\text{-}2}$), the YO transitions to the committed state, in which ecdysteroid production increases further and the YO becomes insensitive to MIH, CHH, and LBA (Chang and Mykles, 2011; Mykles, 2001; Nakatsuji et al., 2009). Increased phosphodiesterase (PDE) activity contributes to the reduced response to MIH by keeping intracellular cyclic nucleotides low (Chang and Mykles, 2011; Nakatsuji et al., 2009). By the end of premolt (stage $D_{3\text{-}4}$), high ecdysteroids initiate the transition from the committed state to the repressed state; hemolymph ecdysteroid titers drop precipitously and the animal molts (Chang and Mykles, 2011; Mykles, 2011).

The signaling pathways that drive the changes in the YO during the premolt period are poorly understood. In insects, the insulin/mechanistic target of rapamycin (mTOR) signal transduction pathway regulates prothoracic gland (PG) growth and ecdysteroidogenic capacity (see (Danielsen et al., 2013; Nijhout et al., 2014; Rewitz et al., 2013; Yamanaka et al., 2013) for reviews). mTOR is a protein kinase highly conserved among the Metazoa that functions as a sensor for cellular growth regulation by nutrients, cellular energy status, oxygen level, and growth factors (Albert and Hall, 2015; Cetrullo et al., 2015; Laplante and Sabatini, 2013). Prothoracicotropic hormone (PTTH) and insulin-like peptides (ILPs) activate mTOR, which phosphorylates p70 S6 kinase (S6K) and eIF4E-binding protein to increase global translation of mRNA into protein (Smith et al., 2014; Teleman, 2010; Yamanaka et al., 2013). FK506-binding protein 12 complexes with rapamycin to inhibit mTOR (Hausch et al., 2013). Binding of ILP to a membrane receptor activates a signal transduction cascade involving PI3K, PDK1, and Akt protein kinases (Teleman, 2010). mTORC1 is activated by Rheb-GTP and is inactivated when Rheb-GTPase activating protein (Rheb-GAP or tuberous sclerosis complex 1/2) promotes the hydrolysis of GTP to GDP by Rheb (Huang and Manning, 2008). Phosphorylation by Akt inactivates Rheb-GAP; the higher Rheb-GTP levels keep mTOR in the active state (Teleman, 2010). Over-expressing Rheb-GAP inhibits PG growth, while over-expressing PI3K, an upstream activator of Akt, stimulates PG growth (Colombani et al., 2005; Layalle et al., 2008; Mirth et al., 2005). In addition, inhibition of PI3K and mTOR blocks the PTTH-dependent increase in ecdysteroid secretion in the PG (Gu et al., 2012; Gu et al., 2011). In *G. lateralis*, rapamycin inhibits YO ecdysteroid secretion *in vitro* and the expression of *Gl-mTOR* and *Gl-Akt* is increased in animals induced to molt by multiple leg autotomy, suggesting that mTOR signaling is involved in YO activation (Abuhagr et al., 2014b).

The transforming growth factor-β (TGF-β) superfamily is mediated by Smad transcription factors that regulate genes through transcriptional activation or repression (Heldin and Moustakas, 2012; Macias et al., 2015; Xu et al., 2012). TGFβ/Smad signaling controls PTTH-stimulated ecdysteroidogenesis in the insect PG (Rewitz et al., 2013; Yamanaka et al., 2013). Disruption of activin (Actb) signaling in *Drosophila* blocks the metamorphic molt by preventing the ecdysteroid peak by PTTH (Gibbens et al., 2011). Activin is required for the PG to respond to PTTH; animals do not molt until they have achieved a critical weight (Rewitz et al., 2013). An activin-like peptide may have a similar function in crustaceans, as the committed YO shows a sustained constitutive increase in ecdysteroid synthesis and reduced sensitivity to MIH (Chang and Mykles, 2011; Nakatsuji et al., 2009).

The components of the mTOR and TGF-β signaling pathways are well represented in the *G. lateralis* YO transcriptome (Das et al., 2016). The purpose of this study is to investigate the roles of mTOR and TGF-β signaling in regulating YO ecdysteroidogenesis. ESA was used to induce molting in *G. lateralis*. The effects of rapamycin, an mTOR inhibitor, on hemolymph ecdysteroid titer and of SB431542, an activin receptor antagonist, on ecdysteroid titer and gene expression *in vivo* were determined. Hemolymph ecdysteroid titer was quantified by competitive ELISA. mRNA levels of *Gl-elongation factor 2* (*Gl-EF2*), *Gl-myostatin-like factor* (*Gl-Mstn*), *Gl-mTOR*, *Gl-Rheb*, *Gl-Akt*, and *Gl-S6k* were quantified by quantitative polymerase chain reaction (qPCR). The results suggest that mTOR and activin signaling control YO ecdysteroidogenesis during premolt.

2. Materials and methods

2.1. Animals and experimental treatments

Adult blackback land crabs, *G. lateralis*, were collected in the Dominican Republic, shipped via commercial air cargo to Colorado, USA, and maintained as described previously (Covi et al., 2010). Molting was induced by eyestalk ablation (Covi et al., 2010; MacLea et al., 2012).

The effects of SB431542 and rapamycin were determined *in vivo*. At Day 0, intermolt *G. lateralis* were ES-ablated and received a single injection of 10 mM SB431542 (Selleck Chemicals, Houston, TX, USA) or 10 mM rapamycin (Selleck Chemicals) in dimethyl sulfoxide (DMSO; ~10 μM estimated final hemolymph concentration) or dimethyl sulfoxide (DMSO; ~0.1% estimated final hemolymph concentration). Intact intermolt animals also received SB431542 or DMSO. The injection volume was based on an estimated hemolymph volume of 30% of the wet weight. It was calculated using the equation: g wet weight × 0.3 µl 10 mM SB431542, 10 mM rapamycin, or DMSO. YOs were harvested at 0, 1, 3, 5 (*Gl-Mstn* only), 7, and 14 days post-injection, frozen in liquid nitrogen, and stored at -80 ˚C. Hemolymph samples (100 μl) were taken at the time of tissue harvesting, mixed with 300 μl methanol, and ecdysteroid was quantified by ELISA (Abuhagr et al., 2014a).

2.2. Expression of mTOR signaling genes in Y-organ

Total RNA was isolated from YOs using TRIzol reagent (Life Technologies, Carlsbad, CA) as described previously (Covi et al., 2010). First-strand cDNA was synthesized using 2 μg total RNA in a 20 μl total reaction with SuperScript III reverse transcriptase (Life Technologies) and oligo-dT(20)VN primer (50 μmol/l; IDT, Coralville, IA) as described (Covi et al., 2010).

A LightCycler 480 thermal cycler (Roche Applied Science, Indianapolis, IN) was used to quantify levels of *Gl-EF2* (GenBank AY552550), *Gl-Mstn* (EU432218), *Gl-mTOR* (HM989973), *Gl-Rheb* (HM989970), *Gl-Akt* (HM989974), and *Gl-S6k* (HM989975) mRNAs (Covi et al., 2008, 2010; MacLea et al., 2012). Reactions consisted of 1 μl first strand cDNA or standard, 5 μl 2× SYBR Green I Master mix (Roche Applied Science), 0.5 μl each of 10 mM forward and reverse primers synthesized by Integrated DNA Technologies (IDT; Coralville, Iowa; Table 1), and 3 μl nuclease-free water. PCR conditions were as follows: an initial denaturation at 95 ºC for 5 min, followed by 45 cycles of denaturation at 95 ˚C for 10 s, annealing at 62 ˚C for 20 s, and extensions at 72 ˚C for 20 s, followed by melting curve analysis of the PCR product. Transcript concentrations were determined with the LightCycler 480 software (Roche, version 1.5) using a series of dsDNA gene standards produced by serial dilutions of PCR product for each gene (10 ag/μl to 10 ng/μl). The absolute amounts of transcript in copy numbers per μg of total RNA in the cDNA synthesis reaction were calculated based on the standard curve and the calculated molecular weight of dsDNA products.

2.3. Statistical analyses and software

Statistical analysis was performed using JMP 12.1.0 (SAS Institute, Cary, NC). Means were compared using one-way analysis of variance (ANOVA), both within and between treatments. *Post-hoc* Tukey tests were additionally used to compare means over time within a treatment group. Data are presented as mean ± 1 S.E. and the level of significance for the all of the data analyses was set at $\alpha = 0.05$. All qPCR data was log transformed to reduce the variance of the mean. The data were graphed using QtiPlot 0.9.9-rc16 (Ion Vasilief, Romania) and adjusted using Adobe Illustrator CC 2015.

3. Results

3.1. Effects of rapamycin on YO ecdysteroidogenesis

Hemolymph ecdysteroid titers are a function of YO ecdysteroid synthetic activity (Chang and Mykles, 2011; Mykles, 2011). ESA caused a significant increase in hemolymph ecdysteroid titer in control animals (vehicle only), starting at 1 day post-ESA (Fig. 1). At 7-14 days post-ESA the animal transitions from early premolt (stage D_0) to mid premolt (stage D_1) (Covi et al., 2010), resulting in a large increase in hemolymph ecdysteroid titer from 7 days post-ESA to 14 days post-ESA (Fig. 1). A single injection of rapamycin at Day 0 blocked the ESA-induced increase in hemolymph ecdysteroid titer, starting at 1 day post-ESA (Fig. 1). Titers increased from Day 3 to Day 14 post-ESA, but the titers were significantly lower than those in control animals at 1, 3, 7, and 14 days post-ESA (Fig. 1).

3.2. Effects SB431542 on YO ecdysteroidogenesis and gene expression

Intact and ESA animals were injected with SB431542 or DMSO at Day 0 and hemolymph and YOs were harvested 1, 3, 7, and 14 days post-injection. There was no effect of SB431542 or DMSO on hemolymph ecdysteroid titers in intact intermolt animals (Fig. 2A). ESA animals injected with DMSO showed a significant increase in hemolymph ecdysteroid titers by 1 day post-ESA; titers continued to increase as the animal progressed through the premolt stage (Fig. 2A). SB431542 had no effect on the initial increase in ecdysteroid titer at 1 and 3 days post-ESA, paralleling the increase in the control ESA animals (Fig. 2A). However, ecdysteroid titers in SB431542-injected ESA animals at 7 and 14 days post-injection were significantly lower than those of the control ESA animals (Fig. 2A). The ecdysteroid titer at 14 days post-ESA was

188 higher than that at 7 days post-ESA, which indicates some recovery from the effects of the
189 reagent (Fig. 2A).
190 ESA-induced increases in YO gene expression in control animals was blunted by
191 SB431542. *Gl-mTOR*, *Gl-Akt*, and *Gl-S6K* mRNA levels were increased in control animals by 3
192 days post-ESA (Fig. 2C, E, F). The increases from Day 0 and Day 3 were 5.9-fold for *Gl-mTOR*;
193 1.3-fold for *Gl-Akt*, and 7.2-fold for *Gl-S6K*; the 2.4-fold increase for *Gl-Rheb* was not
194 significant ($P = 0.25$). There was no significant effect of ESA on *Gl-EF2* and *Gl-Rheb* mRNA
195 levels in control animals (Fig. 2B, D). In contrast to the control ESA animals, gene expression in
196 YOs from SB431542-injected ESA animals either did not change significantly (*Gl-EF2*, *Gl-*
197 *mTOR*, *Gl-Akt*, and *Gl-S6k*; Fig. 2B, C, E, F) or decreased (*Gl-Rheb*; Fig. 2D) at 3 days post-
198 ESA. At Day 1, there were no significant differences in the means of all five genes between the
199 control and SB431542 ESA animals (Fig. 2B-F). The means of the *Gl-EF2*, *Gl-mTOR*, and *Gl-*
200 *Rheb* mRNA levels between control and SB431542 ESA animals were significantly different at 3
201 days and 7 days post-ESA (Fig. 2B, C, D). The means of the *Gl-Akt* mRNA levels were
202 significantly different at 3 days post-ESA (Fig. 2E). There were no significant differences in the
203 means of the *Gl-S6k* mRNA levels between control and experimental treatments at all time
204 intervals (Fig. 2F). The transcript levels between control and experimental treatments converged
205 at 14 days post-ESA for all five genes (Fig. 2B-F). In intact animals, SB431542 had no effect on
206 gene expression (data not shown).
207
208 *3.3. Effects of ESA on expression of Gl-Mstn*
209 Gl-myostatin-like factor (Gl-Mstn) is an activin-like member of the TGF-β family (Covi et
210 al., 2008). It was expressed in all 11 tissues examined, including the YO (Fig. 3). *Gl-Mstn* is the

211 only activin-like contig identified in the *G. lateralis* YO transcriptome (Das et al., 2016).
212 Moreover, as SB431542 blocked the effects of ESA, *Gl-Mstn* mRNA level was quantified to
213 assess its role in the timing of the transition of the activated YO in early premolt to the
214 committed YO in mid premolt. Animals were ES-ablated and injected with DMSO (~0.1% final
215 concentration) at Day 0 to replicate the control treatment in the rapamycin and SB431542
216 injection experiments. YOs were harvested 0 to 14 days post-ESA; a 5-day post-ESA was added
217 for greater temporal resolution before the early to mid premolt transition. ESA resulted in a
218 significant increase in ecdysteroid titer by 3 days post-ESA, but there was no further increase in
219 titers at 7 and 14 days post-ESA, as observed in the controls in the rapamycin/DMSO and
220 SB431542/DMSO injection experiments (compare Fig. 4A with Figs. 1 and 2A). ESA had little
221 effect on *Gl-EF2* mRNA level; the only significant difference was between the means at 1 day
222 and 14 days post-ESA (Fig. 4B). By contrast, *Gl-Mstn* mRNA increased 5.5-fold to its highest
223 level at 3 days post-ESA, then decreased 50-fold over the next 4 days to its lowest level at 7 days
224 post-ESA (Fig. 4C). By 14 days post-ESA, the *Gl-Mstn* mRNA level was comparable to that at
225 1, 3, and 5 days post-ESA, but was significantly higher than the level at Day 0 (Fig. 4C).
226
227 **4. Discussion**
228 The highly conserved mTOR signaling pathway is found in all metazoans and has an
229 important role as a nutrient sensor critical for growth and development in insects (Albert and
230 Hall, 2015; Danielsen et al., 2013; Yamanaka et al., 2013). mTOR mediates the PTTH-induced
231 increase in ecdysteroid synthesis and secretion by the insect PG that triggers molting (Nijhout et
232 al., 2014). mTOR signaling appears to have an analogous role in the crustacean YO. Rapamycin
233 and cycloheximide inhibit ecdysteroid secretion by YOs *in vitro* (Abuhagr et al., 2014b; Mattson

234 and Spaziani, 1986; Mattson and Spaziani, 1987). In *G. lateralis* induced to molt by MLA,
235 mRNA levels of *Gl-mTOR*, *Gl-Akt*, and *Gl-EF2* are increased at premolt stages (Abuhagr et al.,
236 2014b). Acute withdrawal of MIH by ESA increased mRNA levels of *Gl-mTOR*, *Gl-Akt*, and *Gl-*
237 *S6K* in control animals (Fig. 2C, E, F). These data suggest that mTOR-dependent protein
238 synthesis is required for sustained ecdysteroid synthesis in both the insect and crustacean molting
239 glands.

240 In this study, rapamycin blocked YO ecdysteroidogenesis *in vivo*. As the YO cannot store
241 ecdysteroids, the hemolymph ecdysteroid titer is a function of YO ecdysteroidogenic activity
242 (Chang and Mykles, 2011; Mykles, 2011). Molting was induced by ESA and animals were
243 injected with a single dose of rapamycin or vehicle (DMSO) at Day 0. Hemolymph samples were
244 taken at 0, 1, 3, 7, and 14 days post-ESA and hemolymph ecdysteroid was quantified by ELISA.
245 Compared to the control, rapamycin blocked the increase in ecdysteroid titer and the effect lasted
246 for the duration of the experiment (Fig. 1). The prolonged effect of a single injection of
247 rapamycin was probably due to the low solubility of rapamycin in aqueous solutions. A 10 mM
248 rapamycin solution in 100% DMSO was used to keep injection volumes small, so that the final
249 DMSO concentration in the hemolymph did not exceed 0.1%. DMSO at concentrations of 2%
250 and 6% can inhibit YO ecdysteroid secretion (Spaziani et al., 2001). It is likely that much of the
251 rapamycin precipitated at the injection site and apparently took at least 2 weeks to re-dissolve.
252 The sustained release of rapamycin from the injection site inhibited YO ecdysteroidogenesis and
253 prevented, or at least delayed, the further increase in hemolymph ecdysteroid titer from Day 7 to
254 Day 14 post-ESA observed in the control animals (Fig. 1). The higher mean and greater
255 variability in ecdysteroid titer at Day 14 post-ESA in the rapamycin-injected animals suggest that
256 the effect of the drug was beginning to dissipate as the rapamycin was being cleared from the

257 animals (Fig. 1). These data suggest that mTOR activity is required for YO activation and
258 increased ecdysteroid synthesis during the premolt stage. Moreover, mTOR activity appears to
259 be necessary for the transition of the YO from the activated to committed state.
260 The YO undergoes a critical change in physiological properties during the premolt period.
261 In early premolt the activated YO remains sensitive to MIH, CHH, limb autotomy factor -
262 proecdysis (LAF_{pro}), and possibly other signals to suspend molting under unfavorable conditions
263 (Chang and Mykles, 2011; Nakatsuji et al., 2009; Yu et al., 2002). However, during mid premolt
264 the animal makes a decision to complete molting preparations without delay. The YO transitions
265 to the committed state and becomes insensitive to MIH (Chang and Mykles, 2011; Nakatsuji et
266 al., 2009). Molting cannot be suspended by limb bud autotomy (Mykles, 2001; Yu et al., 2002).
267 YO commitment appears to involve Gl-Mstn, an activin-like peptide expressed in the YO (Fig. 3;
268 Das et al., 2016). The increase in *Gl-Mstn* mRNA level coincided with YO activation during the
269 first 3 days post-ESA, followed by a large decrease at 7 days post-ESA (Fig. 4C). Activin
270 receptor antagonist SB431542 caused a delayed decrease in hemolymph titer in ESA animals
271 between 7 and 14 days post-ESA (Fig. 2A). SB431542 had no effect on the initial increase in
272 hemolymph ecdysteroid titer at 1 and 3 days post-ESA, indicating that TGF-β signaling is not
273 required for YO activation. However, the delayed effect of SB431542, as well as the prolonged
274 effect of rapamycin (Fig. 1), suggest that YO activation is prerequisite for YO commitment. The
275 prolonged effect of SB431542 was probably due to its precipitation at the injection site, as the
276 compound, like rapamycin, has low solubility in aqueous solutions. Direct targets of the activin
277 signaling pathway are the mTOR signaling genes and *Gl-EF2*, as SB431542 blocked the increase
278 in *Gl-mTOR* and *Gl-Akt* mRNA levels (Fig. 2C, E) and lowered *Gl-Rheb* and *Gl-EF2* mRNA
279 levels (Fig. 2B, D). The up-regulation of mTOR signaling genes precedes the increase in

ecdysteroidogenesis of the committed YO at Day 7 post-ESA (Fig. 2A). These data are consistent with the hypothesis that the activated YO synthesizes Gl-Mstn for the mid premolt transition and a sustained constitutive increase in ecdysteroid synthesis that is mTOR-dependent.

Activin/Smad signaling may alter expression of genes that determine the committed YO phenotype. Possible downstream targets are genes involved in ecdysteroidogenesis and MIH signaling. The up regulation of Halloween genes, such as *phantom*, is associated with increased ecdysteroid biosynthesis in the YO (Asazuma et al., 2009) and insect PG (Iga and Kataoka, 2012). Down regulation of MIH signaling genes or up regulation of PDEs would reduce sensitivity to MIH (Chang and Mykles, 2011; Nakatsuji et al., 2009). In insects, activin/Smad signaling confers competency to the PG to respond to PTTH to trigger the metamorphic molt (Gibbens et al., 2011; Pentek et al., 2009; Rewitz et al., 2013). These results are the first evidence that an activin-like TGF-β peptide regulates YO ecdysteroidogenesis. As in the insect PG, it may function to alter sensitivity of the YO to neuropeptides.

5. Conclusions

Three signal transduction pathways mediate two critical transitions in the molt cycle of *G. lateralis*. A working model, which incorporates data from this study and from a previous study (Abuhagr et al., 2014b), is illustrated in Figure 5. MIH, via cyclic nucleotide second messengers, maintains the YO in the basal state (Chang and Mykles, 2011; Covi et al., 2009; Webster, 2015). The transition of the YO from the basal to the activated state is initiated by a reduction of circulating MIH (Chang and Mykles, 2011). YO activation involves mTOR-dependent protein synthesis required for cellular growth and increased ecdysteroidogenic capacity, as rapamycin inhibits YO ecdysteroidogenesis *in vitro* (Abuhagr et al., 2014b) and *in vivo* (Fig. 1). A closer

examination of the effects of rapamycin on hemolymph ecdysteroid titer compared to the effects of ESA on mTOR signaling gene expression in control animals suggest that mTOR up regulation involves both transcriptional and posttranslational mechanisms. Initial mTOR activation is likely regulated post-translationally, as the YO is highly sensitive to rapamycin *in vitro* (Abuhagr et al., 2014b) and rapamycin blocked the increase in ecdysteroid titer by 1 day post-ESA (Fig. 1). mTOR is activated by protein phosphorylation and by Rheb through inhibition of the tuberous sclerosis complex (Ekim et al., 2011; Heard et al., 2014; Huang and Manning, 2008). mTOR activation was followed by increased mRNA levels of mTOR signaling genes at 3 days post-ESA (Fig. 2). mTOR regulates gene expression, either directly or indirectly, by phosphorylation of transcription factors, such as STAT3 (Laplante and Sabatini, 2013). mTOR activity may also be required for the transition of the YO from the activated to the committed state, as rapamycin blocked or delayed the large increase in ecdysteroid titer at 14 days post-ESA (Fig. 1).

The model proposes an autocrine regulation by an activin-like peptide that drives the differentiation of the YO to the committed state (Fig. 5). A potential candidate is *Gl-Mstn*, which is expressed in YO, muscle, and other tissues (Fig. 3; Covi et al., 2008; Das et al., 2016). The timing of the peak in *Gl-Mstn* mRNA level (Fig. 4C) and the SB431542-induced drop in mTOR signaling gene mRNA levels at Day 3 and hemolymph ecdysteroid titer at Day 7 (Fig. 2) are consistent with the following mechanism: (1) upon activation, the YO synthesizes and secretes Gl-Mstn peptide through the combination of increased *Gl-Mstn* mRNA and increased mTOR-dependent translation; (2) Gl-Mstn peptide binds to the activin receptor, which phosphorylates and activates R-Smad; and (3) R-Smad binds to Co-Smad and the transcription factor complex translocates to the nucleus and sustains or up regulates genes (e.g., *Gl-EF2*, *Gl-mTOR*, *Gl-Rheb*, and *Gl-Akt*) required for transitioning animals from stage D_0 to D_1 between 7 and 14 days post-

ESA. The model is consistent with the roles of mTOR and activin/Smad signaling in regulating ecdysteroidogenesis in the insect PG (Danielsen et al., 2013; Rewitz et al., 2013; Yamanaka et al., 2013). Current work is using RNA-Seq technology to uncover the gene networks underlying the dynamic changes in YO properties over the molt cycle.

Acknowledgements

We thank Hector C. Horta for collecting *G. lateralis*; Dr. Joseph A. Covi and Kathy Cosenza for technical assistance; and Moriah Echlin, Emily Eisner, Hannah Jesberger, Kent Schnacke, Ryan Shephard, and Rachel Trowbridge for animal care. We acknowledge the staff of the Consejo Dominicano de Pesca y Acuicultura, Dominican Republic, for expediting approval of permits and identifying suitable sites for collecting *G. lateralis*. This research was supported by the National Science Foundation (IOS-0745224 and IOS-1257732).

References

Abuhagr, A.M., Blindert, J.L., Nimitkul, S., Zander, I.A., LaBere, S.M., Chang, S.A., MacLea, K.S., Chang, E.S., Mykles, D.L., 2014a. Molt regulation in green and red color morphs of the crab *Carcinus maenas*: gene expression of molt-inhibiting hormone signaling components. J. Exp. Biol. 217, 796-808.

Abuhagr, A.M., MacLea, K.S., Chang, E.S., Mykles, D.L., 2014b. Mechanistic target of rapamycin (mTOR) signaling genes in decapod crustaceans: Cloning and tissue expression of mTOR, Akt, Rheb, and p70 S6 kinase in the green crab, *Carcinus maenas*, and blackback land crab, *Gecarcinus lateralis*. Comp. Biochem. Physiol. 168A, 25-39.

Albert, V., Hall, M.N., 2015. mTOR signaling in cellular and organismal energetics. Curr. Opinion Cell Biol. 33, 55-66.

Asazuma, H., Nagata, S., Nagasawa, H., 2009. Inhibitory effect of molt-inhibiting hormone on Phantom expression in the Y-organ of the kuruma prawn, *Marsupenaeus japonicus*. Arch. Insect Biochem. Physiol. 72, 220-233.

Cetrullo, S., D'Adamo, S., Tantini, B., Borzi, R.M., Flamigni, F., 2015. mTOR, AMPK, and Sirt1: Key players in metabolic stress management. Crit. Rev. Eukaryotic Gene Expression 25, 59-75.

Chang, E.S., Mykles, D.L., 2011. Regulation of crustacean molting: A review and our perspectives. Gen. Comp. Endocrinol. 172, 323-330.

Colombani, J., Bianchini, L., Layalle, S., Pondeville, E., Dauphin-Villemant, C., Antoniewski, C., Carre, C., Noselli, S., Leopold, P., 2005. Antagonistic actions of ecdysone and insulins determine final size in *Drosophila*. Science 310, 667-670.

Covi, J.A., Bader, B.D., Chang, E.S., Mykles, D.L., 2010. Molt cycle regulation of protein synthesis in skeletal muscle of the blackback land crab, *Gecarcinus lateralis*, and the

364 differential expression of a myostatin-like factor during atrophy induced by molting or
365 unweighting. J. Exp. Biol. 213, 172-183.
366 Covi, J.A., Chang, E.S., Mykles, D.L., 2009. Conserved role of cyclic nucleotides in the
367 regulation of ecdysteroidogenesis by the crustacean molting gland. Comp. Biochem.
368 Physiol. 152A, 470-477.
369 Covi, J.A., Chang, E.S., Mykles, D.L., 2012. Neuropeptide signaling mechanisms in crustacean
370 and insect molting glands. Invert. Reprod. Devel. 56, 33-49.
371 Covi, J.A., Kim, H.W., Mykles, D.L., 2008. Expression of alternatively spliced transcripts for a
372 myostatin-like protein in the blackback land crab, *Gecarcinus lateralis*. Comp. Biochem.
373 Physiol. 150A, 423-430.
374 Danielsen, E.T., Moeller, M.E., Rewitz, K.F., 2013. Nutrient signaling and developmental timing
375 of maturation. In: Rougvie, A.E., O'Connor, M.B. (Eds.), Developmental Timing. Curr.
376 Topics Devel. Biol. 105, 37-67.
377 Das, S., Pitts, N.L, Mudron, M.R., Durica, D.S., Mykles, D.L., 2016. Transcriptome analysis of
378 the molting gland (Y-organ) from the blackback land crab, *Gecarcinus lateralis*. Comp.
379 Biochem. Physiol. 17D, 26-40.
380 Ekim, B., Magnuson, B., Acosta-Jaquez, H.A., Keller, J.A., Feener, E.P., Fingar, D.C., 2011.
381 mTOR kinase domain phosphorylation promotes mTORC1 signaling, cell growth, and
382 cell cycle progression. Molec. Cell. Biol. 31, 2787-2801.
383 Gibbens, Y.Y., Warren, J.T., Gilbert, L.I., O'Connor, M.B., 2011. Neuroendocrine regulation of
384 *Drosophila* metamorphosis requires TGF beta/Activin signaling. Development 138,
385 2693-2703.

386 Gu, S.H., Yeh, W.L., Young, S.C., Lin, P.L., Li, S., 2012. TOR signaling is involved in PTTH-
387 stimulated ecdysteroidogenesis by prothoracic glands in the silkworm, *Bombyx mori*.
388 Insect Biochem. Molec. Biol. 42, 296-303.
389 Gu, S.H., Young, S.C., Tsai, W.H., Lin, J.L., Lin, P.L., 2011. Involvement of 4E-BP
390 phosphorylation in embryonic development of the silkworm, *Bombyx mori*. J. Insect
391 Physiol. 57, 978-985.
392 Hausch, F., Kozany, C., Theodoropoulou, M., Fabian, A.K., 2013. FKBPs and the Akt/mTOR
393 pathway. Cell Cycle 12, 2366-2370.
394 Heard, J.J., Fong, V., Bathaie, S.Z., Tamanoi, F., 2014. Recent progress in the study of the Rheb
395 family GTPases. Cell. Signal. 26, 1950-1957.
396 Heldin, C.H., Moustakas, A., 2012. Role of Smads in TGF beta signaling. Cell Tiss. Res. 347,
397 21-36.
398 Hopkins, P.M., 2012. The eyes have it: A brief history of crustacean neuroendocrinology. Gen.
399 Comp. Endocrinol. 175, 357-366.
400 Huang, J., Manning, B.D., 2008. The TSC1-TSC2 complex: a molecular switchboard controlling
401 cell growth. Biochem. J. 412, 179-190.
402 Iga, M., Kataoka, H., 2012. Recent studies on insect hormone metabolic pathways mediated by
403 cytochrome P450 enzymes. Biol. Pharmaceut. Bull. 35, 838-843.
404 Laplante, M., Sabatini, D.M., 2013. Regulation of mTORC1 and its impact on gene expression at
405 a glance. J. Cell Sci. 126, 1713-1719.
406 Layalle, S., Arquier, N., Leopold, P., 2008. The TOR pathway couples nutrition and
407 developmental timing in *Drosophila*. Dev. Cell 15, 568-577.

408 Macias, M.J., Martin-Malpartida, P., Massague, J., 2015. Structural determinants of Smad
409 function in TGF-beta signaling. Trends Biochem. Sci. 40, 296-308.
410 MacLea, K.S., Abuhagr, A.M., Pitts, N.L., Covi, J.A., Bader, B.D., Chang, E.S., Mykles, D.L.,
411 2012. Rheb, an activator of target of rapamycin, in the blackback land crab, *Gecarcinus*
412 *lateralis*: cloning and effects of molting and unweighting on expression in skeletal
413 muscle. J. Exp. Biol. 215, 590-604.
414 Mattson, M.P., Spaziani, E., 1986. Regulation of Y-organ ecdysteroidogenesis by molt-inhibiting
415 hormone in crabs: involvement of cyclic AMP-mediated protein synthesis. Gen. Comp.
416 Endocrinol. 63, 414-423.
417 Mattson, M.P., Spaziani, E., 1987. Demonstration of protein kinase C activity in crustacean Y-
418 organs and partial definition of its role in regulation of ecdysteroidogenesis. Molec. Cell.
419 Endocrinol. 49, 159-171.
420 Mirth, C., Truman, J.W., Riddiford, L.M., 2005. The role of the prothoracic gland in determining
421 critical weight to metamorphosis in *Drosophila melanogaster*. Curr. Biol. 15, 1796-1807.
422 Mykles, D.L., 2001. Interactions between limb regeneration and molting in decapod crustaceans.
423 Am. Zool. 41, 399-406.
424 Mykles, D.L., 2011. Ecdysteroid metabolism in crustaceans. J. Steroid Biochem. Molec. Biol.
425 127, 196-203.
426 Nakatsuji, T., Lee, C.Y., Watson, R.D., 2009. Crustacean molt-inhibiting hormone: Structure,
427 function, and cellular mode of action. Comp. Biochem. Physiol. 152A, 139-148.
428 Nijhout, H.F., Riddiford, L.M., Mirth, C., Shingleton, A.W., Suzuki, Y., Callier, V., 2014. The
429 developmental control of size in insects. WIREs Dev. Biol. 3, 113-134.

Pentek, J., Parker, L., Wu, A., Arora, K., 2009. Follistatin preferentially antagonizes activin rather than BMP signaling in *Drosophila*. Genesis 47, 261-273.

Rewitz, K.F., Yamanaka, N., O'Connor, M.B., 2013. Developmental checkpoints and feedback circuits time insect maturation. In: Shi, Y.B. (Ed.) Animal Metamorphosis. Curr. Topics Devel. Biol. 103. 1-33.

Smith, W.A., Lamattina, A., Collins, M., 2014. Insulin signaling pathways in lepidopteran ecdysone secretion. Frontiers Physiol. 5, Article 19.

Spaziani, E., Jegla, T.C., Wang, W.L., Booth, J.A., Connolly, S.M., Conrad, C.C., Dewall, M.J., Sarno, C.M., Stone, D.K., Montgomery, R., 2001. Further studies on signaling pathways for ecdysteroidogenesis in crustacean Y-organs. Am. Zool. 41, 418-429.

Teleman, A.A., 2010. Molecular mechanisms of metabolic regulation by insulin in *Drosophila*. Biochem. J. 425, 13-26.

Webster, S.G., 2015. Endocrinology of molting. In: Chang, E.S., Thiel, M. (Eds.), The Natural History of the Crustacea: Physiology, vol. 4. Oxford University Press, Oxford, pp. 1-35.

Xu, P.L., Liu, J.M., Derynck, R., 2012. Post-translational regulation of TGF-beta receptor and Smad signaling. FEBS Lett. 586, 1871-1884.

Yamanaka, N., Rewitz, K.F., O'Connor, M.B., 2013. Ecdysone control of developmental transitions: Lessons from *Drosophila* research. In: Berenbaum, M.R. (Ed.) Ann. Rev. Entomol. 58, 497-516.

Yu, X.L., Chang, E.S., Mykles, D.L., 2002. Characterization of limb autotomy factor-proecdysis (LAF_{pro}), isolated from limb regenerates, that suspends molting in the land crab *Gecarcinus lateralis*. Biol. Bull. 202, 204-212.

Table 1. **Oligonucleotide primers used for gene expression analysis (qPCR).**

Primer	Sequence (5'-3')	Product Size (bp)
Gl-EF2 F1	TTCTATGCCTTTGGCCGTGTCTTCTC	227
Gl-EF2 R1	ATGGTGCCCGTCTTAACCA	
Gl-Mstn F1	GCTGTCGCCGATGAAGATGT	118
Gl-Mstn R1	GGCTGGGGACCTCAATCCCGT	
Gl-mTOR F2	AGAAGATCCTGCTGAACATCGAG	159
Gl-mTOR R2	AGGAGGGACTCTTGAACCACAG	
Gl-Rheb F1	TTTGTGGACAGCTATGATCCC	119
Gl-Rheb R1	AAGATGCTATACTCATCCTGACC	
Gl-Akt F2	AACTCAAGTACTCCAGCGATGATG	156
Gl-Akt R1	GGTTGCTACTCTTTTCACGACAGA	
Gl-s6k F2	GGACATGTGAAGCTCACAGACTTT	239
Gl-s6k R1	TTCCCCTTCAGGATCTTCTCTATG	

Abbreviations: Gl, *G. lateralis*; F, forward; R, reverse; Akt, protein kinase B; EF2, elongation factor 2; Mstn, myostatin-like factor; mTOR, mechanistic target of rapamycin; Rheb, Ras homolog expressed in brain; and s6k, p70 S6 kinase.

Figure Legends

Fig. 1. Effect of mTOR inhibitor rapamycin on hemolymph ecdysteroid titers in *G. lateralis in vivo*. Animals were eyestalk-ablated at Day 0 and injected with a single dose of rapamycin (~10 μM final hemolymph concentration) or equal volume of DMSO (~0.1% final hemolymph volume). Data presented as mean ± 1 S.E. (n = 5-8). Asterisks indicate means that were significantly different ($P < 0.05$) between control and rapamycin at the same time point. Letters indicate significant differences in the means within a treatment (upper case for control; lower case for rapamycin); means that were not significantly different share the same letter.

Fig. 2. Effects of activin receptor antagonist SB431542 on YO ecdysteroidogenesis and gene expression in *G. lateralis in vivo*. Intact and eyestalk-ablated animals were injected with a single dose of SB431542 in DMSO (~10 μM final hemolymph concentration) or DMSO (~0.1% final hemolymph concentration) at Day 0. (A) Hemolymph ecdysteroid titer. Transcript levels of (B) *Gl-EF2*, (C) *Gl-mTOR*, (D) *Gl-Rheb*, (E) *Gl-Akt*, and (F) *Gl-s6k* were quantified by qPCR. Data are presented as mean ± 1 S.E. (sample size for each treatment: Day 0, n = 8; Days 1, 3, and 7, n = 5; Day 14, n = 7). Asterisks indicate means that were significantly different ($P < 0.05$) between control and SB431542 at the same time point. Letters indicate significant differences in the means within a treatment (upper case for control; lower case for SB431542); means that were not significantly different share the same letter. Means without letters were not significantly different at all time points within a treatment. Gene expression in intact animals was not measured (see Materials and methods).

Fig. 3. Tissue expression of *Gl-Mstn* and *Gl-EF2*. End-point RT-PCR was used to qualitatively assess mRNA levels of *Gl-Mstn* and *Gl-EF2* in gill (G), heart (H), heptatopancreas (HP), midgut (MG), hindgut (HG), claw muscle (CM), thoracic muscle (TM), testes (T), thoracic ganglion (TG), Y-organ (YO), and eyestalk ganglia (ESG).

Fig. 4. Effects of eyestalk ablation on hemolymph ecdysteroid titer (A) and *Gl-EF2* (B) and *Gl-Mstn* (C) mRNA levels in *G. lateralis* YO. Animals were ES-ablated and received a single injection of DMSO (~0.1% final concentration) at Day 0. Data are presented as mean ± SEM (Day 0, n = 8; Days 1, 3, 7, and 14, n = 10; Day 5, n = 9). Upper case letters indicate significant differences in the means. Means that were not significantly different share the same letter; the mean without a letter (7 days post-ESA) was significantly different from all other means. Abbreviations: EF2, elongation factor-2; Mstn, myostatin-like factor.

Fig. 5. Proposed model for the regulation of the YO by MIH, mTOR, and TGF-β signaling pathways. Pulsatile release of MIH maintains the YO in the basal state and the animal remains in intermolt. Decreased MIH release triggers mTOR-dependent YO activation, which is inhibited by rapamycin. The activated YO produces an activin-like TGF-β peptide (Mstn), which drives the transition to the committed state in mid premolt. SB431542, an activin receptor antagonist, blocks the transition of the YO from the activated to committed state.

516 **Figure 1**

517

518

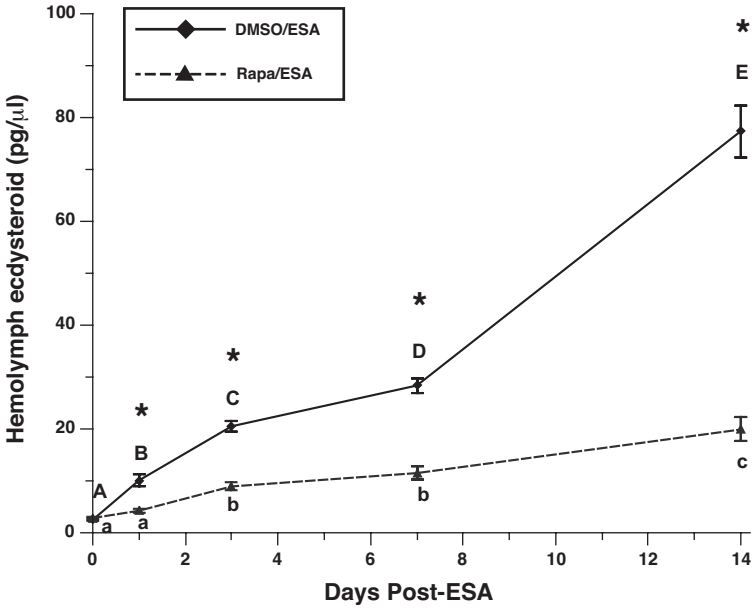

519 **Figure 2**

520

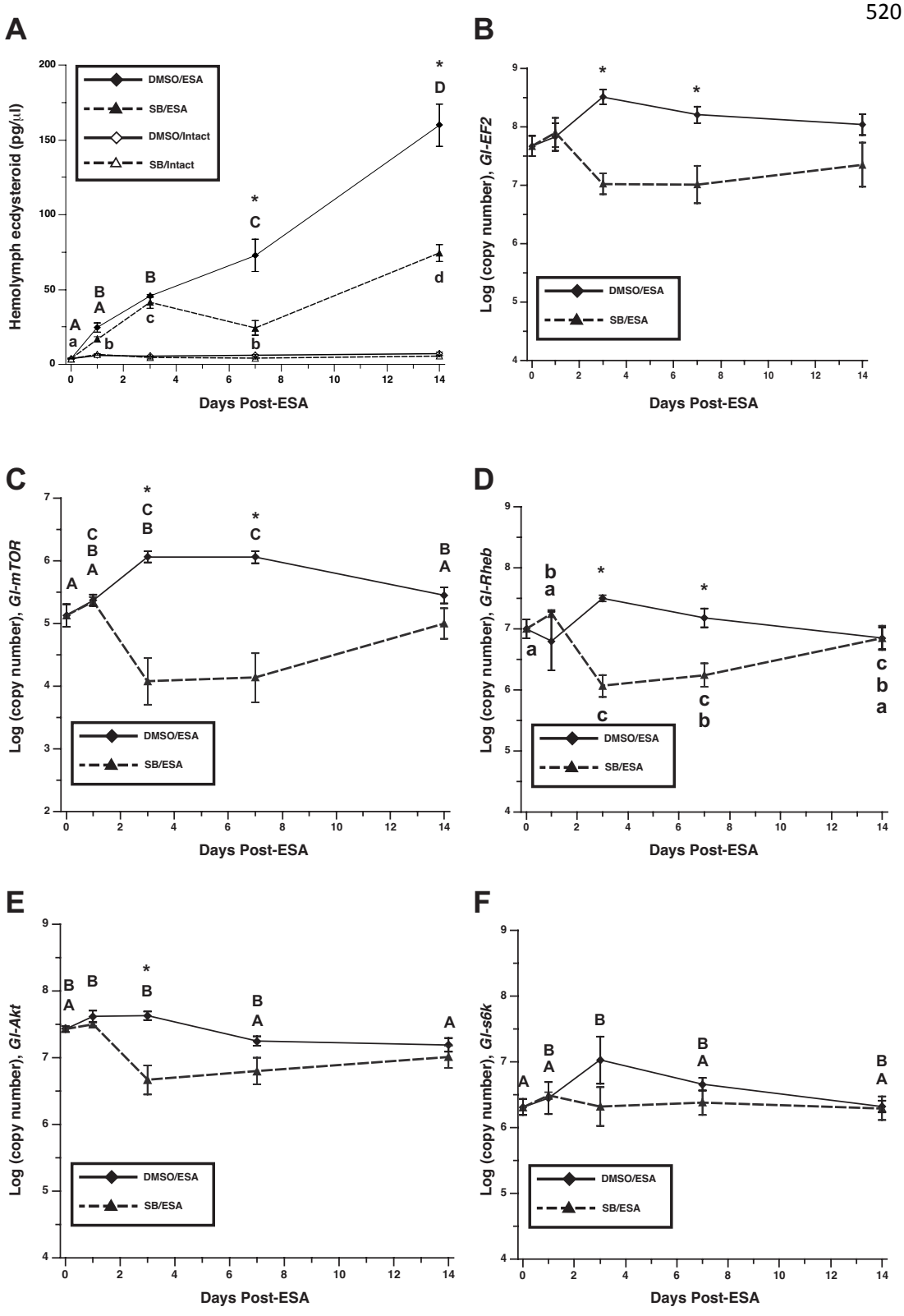

521 **Figure 3**

522

523

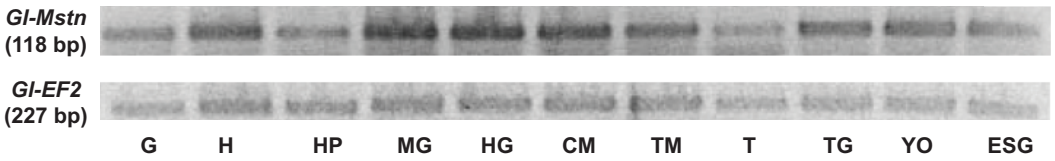

524 **Figure 4**

525

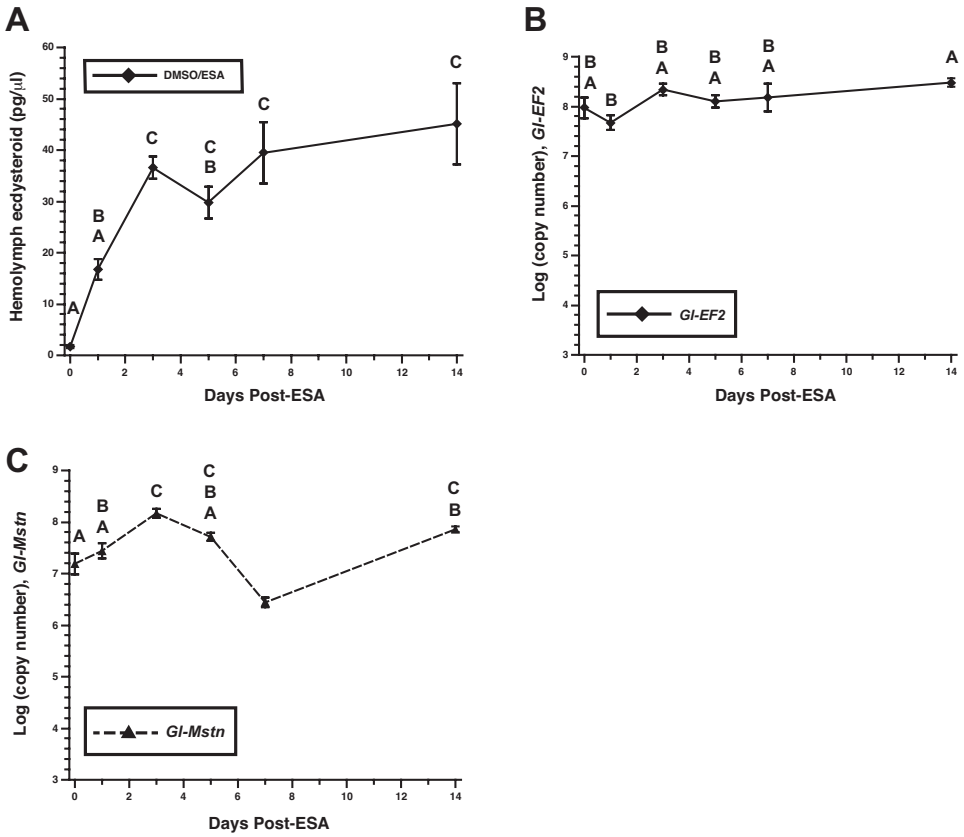

526 **Figure 5**

527